Dynamics of Optoelectronic Oscillators With Electronic and Laser Nonlinearities

Géraud. R. Goune Chengui, Jimmi H. Talla Mbé, Alain Francis Talla, Paul Woafo, and Yanne K. Chembo, *Senior Member, IEEE*

***Abstract*— We present a theoretical and experimental study of a low-frequency optoelectronic oscillator featuring both laser-diode and Van der Pol-like nonlinearities. In this architecture, the device performing the electrical-to-optical conversion is the laser-diode itself instead of an external electro-optical modulator, while the electric branch of the oscillator is characterized by a Van der Pol nonlinear transfer function. We show that the system displays a complex autonomous dynamics, induced by the competition between these two nonlinearities. In the case of small delay, the system displays harmonic and relaxation oscillations. When the delay is large, the interplay between the two nonlinearities leads to a period-doubling route of bifurcations as the feedback gain is increased, and ultimately to fully developed chaos. Our experimental measurements are in good agreement with the theoretical analysis.**

***Index Terms*— Optoelectronic devices, nonlinear oscillators.**

I. Introduction

OPTOELECTRONIC oscillators (OEOs) are autonomous nonlinear systems with a feedback loop constituted with an optical and an electrical branch. In general, these systems are optically seeded by a continuous-wave laser (typically around 800 or 1550 nm) and can output a radio-frequency signal with a frequency range from 1 kHz to 100 GHz. Since the pioneering work of Neyer and Voges [1], OEOs have been the focus of intense research activities from the fundamental viewpoint (see for example [2]–[21]). This interest has also led to many applications in ultra-stable microwave generation [22]–[35], optical communications [36]–[38], or neuromorphic computing [39]–[43], amongst others. A general overview of these applications is provided in [44]. OEOs also emerged as relevant systems for sensing, measurement and detection, as comprehensively reviewed in [45].

Differential Delay Equations (DDEs) are generally used to model these OEOs, and the literature devoted to their nonlinear delay dynamics has been particularly rich [46], [47]. In most cases, the device performing the nonlinear conversion between the electrical and the optical signal in OEOs is a phase or intensity modulator with a sinusoidal transfer function. However, other electro-optic or optoelectronic devices can be used to perform this nonlinear conversion [20], [21], [48], [49], thereby allowing for on-chip miniaturization and integration [31]. For example, in [48], an electroabsorption modulated laser was used to simultaneously perform three operations, namely lasing, photodetection and intensity modulation. A compact architecture in which the intensity modulation of the laser light is performed through a direct optical feedback onto the laser-diode was proposed as well in [49] and [50]. Another alternative to achieve the nonlinear conversion can consist to use the power-intensity - or "PI" - transfer function of the seeding laser diode itself without external cavity. That transfer function is a "piece-wise linear" nonlinearity (function equal to zero below a given threshold current, and linearly increasing above).

On the other hand, OEOs generally have a linear electric branch, where the electric signal is amplified and eventually frequency-filtered. An open point is to investigate the behavior of the OEO when this electric branch responds nonlinearly to an input excitation. The nonlinearity we have chosen for the electric branch is the one of the most standard in electronics, and corresponds to the so-called Van der Pol-like nonlinearity. As a historical note, that nonlinearity is originated from a self-oscillatory system known as the Van der Pol (or VdP) oscillator, introduced by Balthasar Van der Pol in the 1920s. Since then, it has been a very fruitful paradigm for autonomous and relaxation oscillations in physical and biological systems.

It is important to note that the additional nonlinearity is expected to generate novel complex behaviors that do not exist in the conventional OEO architectures, and which have the capability to emulate enhanced functionalities for sensing and

Manuscript received September 6, 2017; revised October 28, 2017 and November 28, 2017; accepted November 29, 2017. Date of publication December 11, 2017; date of current version December 22, 2017. This work was supported by the International Center for Theoretical Physics, Trieste, Italy. *(Corresponding author: Yanne K. Chembo.)*

G. R. Goune Chengui and A. F. Talla are with the Laboratory of Modelling and Simulation in Engineering, Biomimetics and Prototypes, Department of Physics, University of Yaoundé I, Yaoundé 812, Cameroon (e-mail: geraud.goune@yahoo.fr; fratalai@yahoo.fr).

J. H. Talla Mbé is with the Laboratory of Modelling and Simulation in Engineering, Biomimetics and Prototypes, Department of Physics, University of Yaoundé I, Yaoundé 812, Cameroon, and also with the Laboratory of Condensed Matter, Electronics and Signal Processing, Department of Physics, University of Dschang, Dschang 67, Cameroon (e-mail: jhtallam@yahoo.fr).

P. Woafo is with the Laboratory of Modelling and Simulation in Engineering, Biomimetics and Prototypes, Department of Physics, University of Yaoundé I, Yaoundé 812, Cameroon, and also with the Applied Physics Group, Vrije Universiteit Brussel, 1050 Brussel, Belgium (e-mail: pwoafo1@yahoo.fr).

Y. K. Chembo is with the Optics Department, CNRS, Franche-Comté Electronique, Mécanique, Thermique et Optique-Sciences et Technologies Institute, Université Bourgogne Franche-Comté, 25030 Besançon, France, and also with the GeorgiaTech-CNRS Joint International Laboratory [UMI 2958], Atlanta Mirror Site, School of Electrical and Computer Engineering, Atlanta, GA 30332 USA (e-mail: yanne.chembo@femto-st.fr).

Color versions of one or more of the figures in this paper are available online at http://ieeexplore.ieee.org.

Digital Object Identifier 10.1109/JQE.2017.2782319

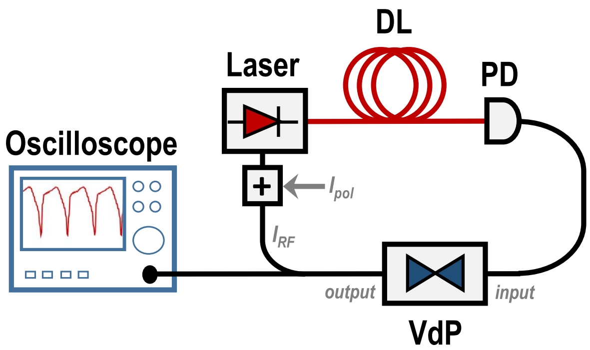

Fig. 1. The experimental set-up of the Van der Pol-optoelectronic oscillator (VdP-OEO). DL: Delay line; PD: Photodiode; I_{pol}: Laser polarization current; I_{RF}: RF current from the feedback loop.

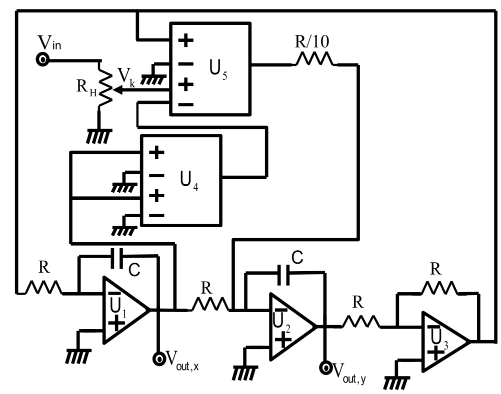

Fig. 2. Experimental set-up of the Van der Pol oscillator. U_1, U_2 and U_3 are operational amplifiers, while U_4 and U_5 are analog multipliers.

information processing. Indeed, even if the original applications of OEOs have mainly been oriented towards microwave generation and optical chaos cryptography, it is known today that OEOs are useful as well for photonic neuromorphic computing [44], and allow for unprecedented performances [43]. In these analog computers, multi-nonlinearity in the feedback loop of the OEO can enhance the computing capabilities of the system. For example, certain tasks require strong coupling between the computing nodes, and such coupling is generally ensured by nonlinear mixing. In this regard, the Van der Pol circuit has been shown to be an ideal element to harness synchrony and memory effects in electronic neuromorphic systems [51]–[54]. Therefore, inserting a Van der Pol circuit into an OEO loop would allow to benefit simutaneously from the large bandwidth of the photonic components, and from the neuromorphic computing advantages of the Van der Pol-like nonlinearity.

In this article, we aim to analyze this OEO where the laser-diode nonlinearity is used to perform the conversion from the electrical to the optical domain, and where the electric branch has a VdP-like nonlinearity. We experimentally build the system and investigate the complex output dynamics of the electric signal in the time-domain. We also propose an explicit nonlinear model to describe this dynamics in Sec. II. The stability of this OEO is analyzed in Sec. III. Numerical simulations for this model are performed and found to be in excellent agreement with our experimental results in Sec. IV. The last section concludes the article.

II. System and Model

Our OEO is displayed in Fig. 1, and is composed of the following elements: (i) A continuous-wave (CW) distributed feedback laser-diode source with telecom wavelength $\lambda = 1550$ nm, threshold current $I_{\text{th}} = 16$ mA, pump current $I_{\text{pol}}+I_{\text{RF}}(t)$ and output power $P(t)$, where I_{pol} is the polarization current, $I_{\text{RF}}(t)$ is the time-varying radio-frequency (RF) current, and $P(t)$ can be varied from 0 to 10 mW; (ii) An optical fiber cable with length L, yielding a time-delay $T_D = nL/c$ where $n = 1.5$ is the group velocity refraction index of the fiber, and c is the velocity of light in vacuum; (iii) An InGaAs photodiode (PD) with responsivity $S = 4.75$ V/mW at 1550 nm and detection bandwidth of 100 MHz. This photodiode converts the incoming power into an electric voltage $V(t)$, which interacts with a VdP oscillator before being converted back into a current $I_{\text{RF}}(t)$ that is used to pump the laser-diode.

The electric circuit corresponding to the VdP oscillator is explicitly shown in Fig. 2. The main components are: The resistor $R = 10$ kΩ; The capacitor $C = 10$ nF; The potentiometer R_{H} with maximal resistance equal to $R_{\text{H}_{\text{max}}} = 100$ kΩ; The operational amplifiers U_1, U_2 and U_3 (type LF356); The analog multipliers U_4 and U_5 (type AD633) with differential inputs and divide-by-ten outputs. It is important to note that, even though oscillators are in principle autonomous, our VdP circuit features an input and an output port, and is therefore inserted here as a nonlinear dipole in the delayed feedback loop.

The electronic circuit is described by the following set of equations:

$$\frac{dV_{\text{out},x}}{dt} = \frac{1}{RC}V_{\text{out},y} \tag{1}$$

$$\frac{dV_{\text{out},y}}{dt} = -\frac{1}{RC}V_{\text{out},x} + \frac{k_m}{RC}\left[k_p K_d V_{\text{in}} - K_d^2 V_{\text{out},x}^2\right] V_{\text{out},y} \tag{2}$$

where $k_m = 10$ is a dimensionless constant corresponding to the fact that the resistance at the output of U_5 is equal to $R/10$, $k_p = 1 - R_{\text{H}}/R_{\text{H}_{\text{max}}}$ is a dimensionless proportionality constant from the potentiometer R_{H} (continuously tunable from 0 to 1), $K_d = 0.1$ V^{-1} is the proportionality factor of the multipliers, and V_{in} is the input voltage. Let us introduce the dimensionless time

$$\tau = \frac{t}{RC} \tag{3}$$

and the dimensionless voltages

$$x = \sqrt{k_m} \quad K_d V_{\text{out},x} \tag{4}$$

$$y = \sqrt{k_m} \quad K_d V_{\text{out},y}. \tag{5}$$

By combining Eqs. (1) and (2), we find that the dynamical state of the circuit obeys the following dimensionless autonomous equation

$$\ddot{x} - (\varepsilon - x^2)\dot{x} + x = 0, \tag{6}$$

with $\varepsilon = k_m k_p K_d V_{\text{in}}$ being the dimensionless gain of the oscillator when the voltage V_{in} is held constant, while the over-dot stands for the derivative with respect to the dimensionless time τ. In the above equation, the transformation $x \to x/\sqrt{\varepsilon}$ yields the original VdP equation of the form

$$\ddot{x} - \varepsilon(1 - x^2)\dot{x} + x = 0, \tag{7}$$

but we prefer the form of Eq. (6) because in our case, it allows to understand better the effect of the VdP-like nonlinearity $[(\varepsilon - x^2)\dot{x}]$ in the OEO feedback loop. It is well known that as its gain increases, a solitary VdP system undergoes a Hopf bifurcation towards a stable limit-cycle with quasi-sinusoidal oscillations. In our circuit, the frequency of the Hopf limit-cycle is $\omega_0 = 1/RC = 2\pi \times 1.59$ kHz. As the gain is further increased, the harmonic oscillations change into relaxation oscillations characterized by a slow-fast dynamics.

One of the most important component of our OEO is the laser-diode, which performs the conversion from the electric to the optical domain. The dimensionless nonlinear transfer function of the laser diode is

$$\mathrm{D}(x) = x\mathrm{H}(x) = \frac{1}{2}[x + |x|] = \begin{cases} 0 & \text{for } x \leq 0 \\ x & \text{for } x > 0, \end{cases} \tag{8}$$

where $\mathrm{H}(x)$ is the well-known Heaviside step-function which is equal to 0 for $x \leq 0$ and to 1 otherwise. Accordingly, the diode nonlinearity function $\mathrm{D}(x)$ is null for negative x, and is equal to x otherwise (linear increase).

In laser-diodes, the nonlinear transfer function is usually of the form $\mu\mathrm{D}(I - I_{\text{th}})$, which is equal to 0 for $I < I_{\text{th}}$, and equal to $\mu(I - I_{\text{th}})$ for $I \geq I_{\text{th}}$. The parameter $\mu = \eta_d h\nu$ is the laser conversion slope, with η_d being the quantum efficiency, h the Planck constant, and ν the laser carrier frequency. We have experimentally determined that $\mu = 0.21$ mW/mA for our laser. Hence, if we set $I_0 = I_{\text{th}} - I_{\text{pol}}$, the power-intensity (PI) transfer function of our laser-diode is therefore $P(t) = \mu\mathrm{D}[I_{\text{RF}}(t) - I_0]$, or equivalently,

$$P(t) = \begin{cases} 0 & \text{for } I_{\text{RF}}(t) \leq I_0 \\ \mu[I_{\text{RF}}(t) - I_0] & \text{for } I_{\text{RF}}(t) > I_0. \end{cases} \tag{9}$$

It is important to note that here, even in the case where the pump current and laser power are time dependent, it is legitimate to discard the internal dynamics of the laser (coupled equations for carrier and photon density) and consider that the output power $P(t)$ adiabatically follows the pump current $I(t)$ via the nonlinear function D. This is possible because our oscillations are expected to be of the order of kHz, that is, much slower than the intrinsic GHz laser dynamics: otherwise, we should have to account for the laser intracavity photons and carrier dynamics [55]. The optical output power P is then converted into the electrical domain through the photodiode (PD), according to the relation $V(t) = SP(t - T_D)$, where T_D is the time-delay originating from the propagation time in the fiber line between the laser and the photodetector, and S the responsivity of the photodiode. The input voltage used to polarize the VdP circuit can therefore be written as

$$V_{\text{in}}(t) = \kappa V(t) = \kappa S\mu\mathrm{D}[I_{\text{RF}}(t - T_D) - I_0], \tag{10}$$

where κ is a dimensionless factor standing for all the linear losses (electrical and optical) in the feedback loop. Finally, the output voltage $V_{\text{out}} \equiv V_{\text{out},x}$ is converted to the current $I_{\text{RF}}(t) = V_{\text{out},x}(t)/R_Z$, where $R_Z = 50\ \Omega$ is the characteristic impedance used for the voltage-to-intensity conversion. Neglecting the electrical delay and considering only the optical one, our VdP-OEO is described by the autonomous delay equation

$$\ddot{x} - [\beta\mathrm{D}(x_T - \alpha) - x^2]\dot{x} + x = 0, \tag{11}$$

where $T = \omega_0 T_D$ is the dimensionless delay,

$$\beta = \mu\kappa S k_p \sqrt{k_m}/R_Z \tag{12}$$

is the dimensionless gain, and

$$\alpha = \sqrt{k_m} K_d R_Z I_0 \tag{13}$$

is the dimensionless offset value for the diode nonlinearity, while we still have $x = \sqrt{k_m} K_d V_{\text{out},x}$, and the time delay variable $x_T = x(\tau - T)$. The VdP-OEO described by Eq. (11) degenerates to the usual VdP equation presented in Eq. (6) if one replaces the diode function $\mathrm{D}(x_T - \alpha)$ by a constant.

III. Stability Analysis

In order to understand the dynamics of this nonlinear system, it is useful to determine the fixed points of the system, and to investigate their stability. The dynamical Eq. (11) can be rewritten under the form of the following flow

$$\dot{x} = y \tag{14}$$
$$\dot{y} = -x + [\beta\mathrm{D}(x_T - \alpha) - x^2]y. \tag{15}$$

Finding the fixed point requires to set all the time-derivatives to zero, and we obtain the unique solution $(x_0, y_0) = (0, 0)$, which is the trivial fixed point. In order to investigate its stability, this fixed point has to be perturbed as $(x, y) = (x_0 + \delta x, y_0 + \delta y)$, and we have to determine the asymptotic behavior of the perturbations. It can be shown that the perturbation flow can be explicitly written as

$$\delta\dot{x} = \delta y \tag{16}$$
$$\delta\dot{y} = -\delta x + \beta\mathrm{D}(-\alpha)\delta y, \tag{17}$$

which is independent of the delay because of the mathematical properties of the nonlinear function D. The perturbations can be considered as dependent on the eigenvalue λ following $\delta x(\tau) \propto e^{\lambda\tau}$ and $\delta y(\tau) \propto e^{\lambda\tau}$, and by inserting these approximations into Eqs. (16) and (17), we obtain the characteristic equation

$$\lambda^2 - \beta\mathrm{D}(-\alpha)\lambda + 1 = 0. \tag{18}$$

The solutions of this eigenvalue equation are

$$\lambda_{\pm} = \frac{1}{2}\left[\beta\mathrm{D}(-\alpha) \pm \sqrt{\beta^2\mathrm{D}^2(-\alpha) - 4}\right], \tag{19}$$

and we find that the stability of the system critically depends on the value of the parameter α.

In the case when $\alpha \geq 0$ (or $I_{\mathrm{pol}} \leq I_{\mathrm{th}}$), we have $\mathrm{D}[-\alpha] \equiv 0$, and the solutions for the eigenvalue equation are

$$\lambda_{\pm} = \pm i. \tag{20}$$

The fixed point is in this case a *center*, which is topologically equivalent to the fixed point of the harmonic oscillator. This situation of neutral stability is such that the nature and magnitude of the nonlinear terms are of critical importance at the time to determine the behavior of the full system.

On the other hand, when $\alpha < 0$ (or $I_{\mathrm{pol}} > I_{\mathrm{th}}$), we have $\mathrm{D}[-\alpha] \equiv -\alpha$, and the solutions for the eigenvalue equation are

$$\lambda_{\pm} = \frac{1}{2}\left[-\alpha\beta \pm \sqrt{\alpha^2\beta^2 - 4}\right], \tag{21}$$

which is such that the real parts of the eigenvalues are positive. The fixed point is therefore in this case an *unstable node* or an *unstable focus*, and this configuration corresponds to the typical case of a Van der Pol oscillator. The expected phenomenology is that in the phase portrait, this unstable trivial fixed point should be surrounded by a stable limit-cycle.

IV. Periodic and Chaotic Dynamics

The setup described in Fig. 1 is used to record and analyze the oscillating waveforms observed under different values of the gain which is varied through k_p for the experimental measurements, and through β (which is proportional to k_p) for numerical simulations. In the experiment, the tuning of the potentiometer R_{H} gives the range of V_{in} from 0 to 3.38 V. The polarization voltage is taken as $V_{\mathrm{th}} - V_{\mathrm{pol}} = 1.31$ V in order to allow the laser to reach its linear region.

We first consider the case of short delay. The length of the optical fiber cable is $L = 42$ m, yielding a time-delay $T_D = 0.21$ μs. The dimensionless delay $T = \omega_0 T_D \sim 10^{-3}$ is significantly smaller compared to the time scale τ. Consequently, the delay term $x_T = x(\tau - T)$ does not greatly affect the dynamics of the system, which therefore becomes two-dimensional for all practical purposes. According to the Poincaré-Bendixon theorem, the attractors are necessarily either fixed points or limit-cycles. In Fig. 3, it can be seen that for low gain, one obtains a quasi-sinusoidal oscillation after the Hopf bifurcation. As the gain is increased, we observe a significant qualitative deviation from the harmonic behavior. Figure 3 also unveils that as the voltage V_k (or k_p) is increased, the period of the oscillations increases as well. The good agreement between the experimental results and the numerical simulations validates the theoretical analysis. The main difference between the VdP and the VdP-OEO is that oscillations in the latter case are asymmetric, with a skewness towards positive values. Along the same line, the transitions from negative to positive values are slower than those from positive to negative in the VdP-OEO, while both transitions are of equal duration in the classical VdP oscillator.

For large delay (for instance, $T = 4$), the delay term $x_T = x(\tau - T)$ considerably differs from x, and independently affects the dynamics of the system. In particular, the dimensionality of the oscillator increases dramatically, thereby allowing the emergence of different types of attractors, including chaotic ones. This complex behavior results from the interplay of the delay and the two nonlinearities of the system (originating from the laser-diode and the Van der Pol circuit). It should be noted that such large delays do not need to be exclusively induced by the delay line, and instead,

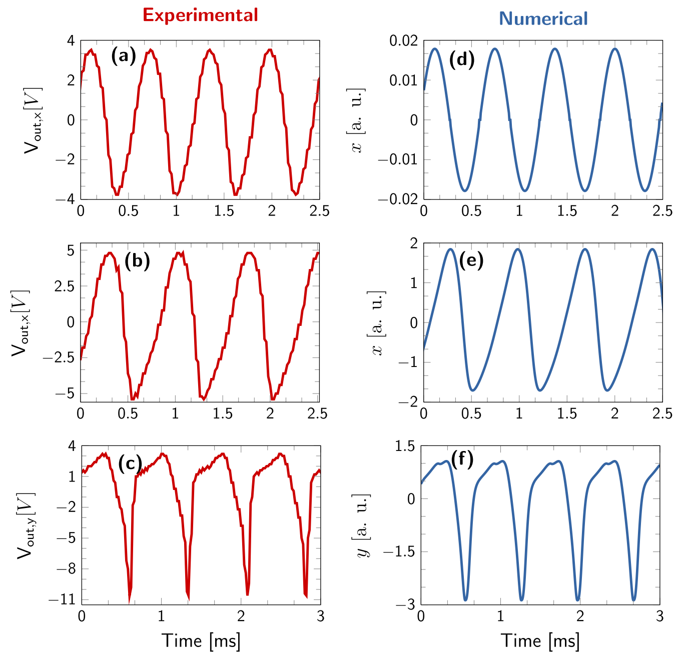

Fig. 3. Temporal evolution of the VdP-OEO. Left column [(a), (b) and (c)]: experimental measurements for $R = 10$ kΩ, $C = 10$ nF, $T_D = 0.21$ μs and $V_{\mathrm{th}} - V_{\mathrm{pol}} = 1.314$ V, when the gain is varied through k_p. Right column: corresponding numerical simulations from Eq. (11) for $T = 2.1 \times 10^{-3}$ and $\alpha = 0.1$, when β is varied. (d) x for $\beta = 1.2$; (e) x for $\beta = 2.2$; (f) y for $\beta = 2.2$.

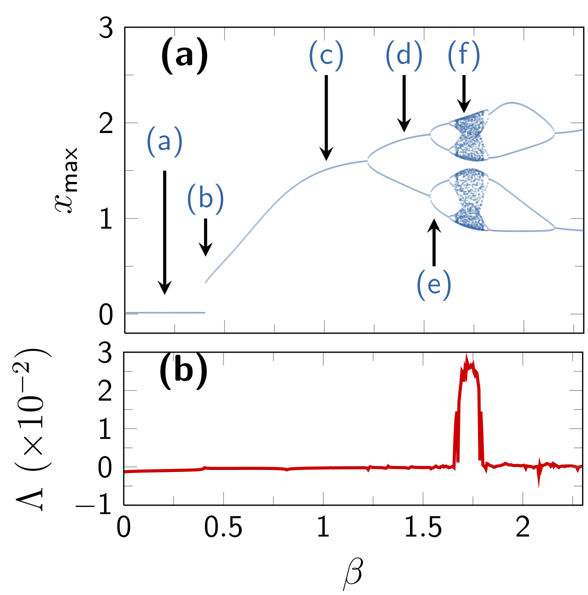

Fig. 4. (a) Numerical plots of the bifurcation diagram for the variable x (maxima). (b) Lyapunov exponent Λ of the system for $T = 4$ and $\alpha = 0.1$. The labels (a)–(f) indicate the dynamical regimes corresponding to the phase portraits of Fig. 5.

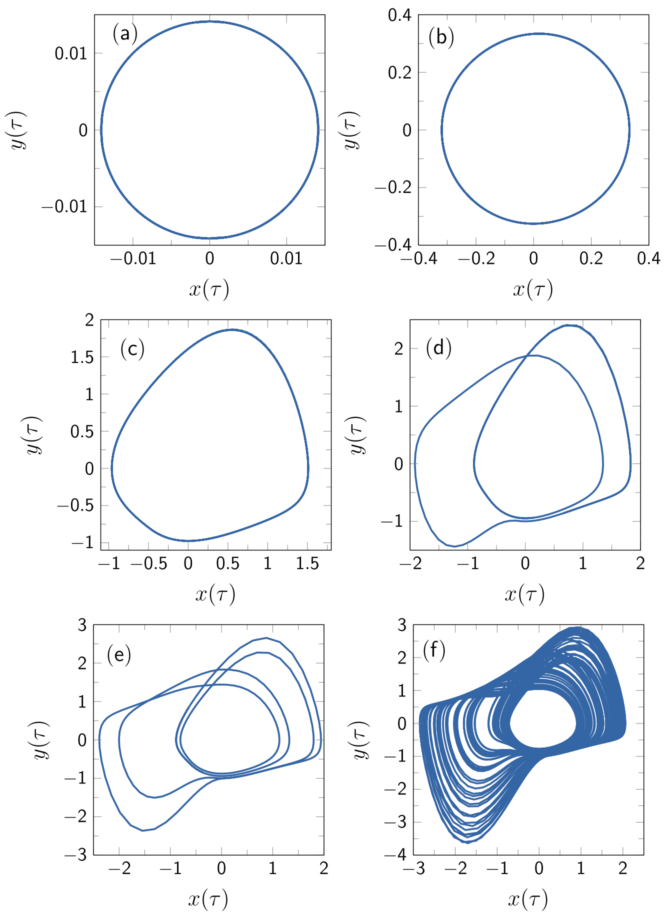

Fig. 5. Numerical simulations of Eq. (11) for $T = 4$ and $\alpha = 0.1$ of the VdP-OEO for various gain values β in phase space. These phase portraits correspond to the operating points highlighted in Fig. 4(a). (a) $\beta = 0.2$: Quasi-sinusoidal oscillations with low amplitudes. (b) $\beta = 0.405$: Quasi-sinusoidal with high amplitude. (c) $\beta = 1.01$: Non-sinusoidal with high amplitudes. (d) $\beta = 1.4$: Period-two oscillations. (e) $\beta = 1.55$: Period-four oscillations. (f) $\beta = 1.7$: Chaos.

they can be implemented electronically using for example digital signal processing (DSP) boards [5]. Figure 4(a) displays a numerical bifurcation diagram from Eq. (11) as the gain parameter β is increased with $\alpha = 0.1$ and $T = 4$ (held fixed). One can observe the classical cascade of frequency-doubling bifurcations leading to fully developed chaos. In order to unambiguously quantify the occurrence of chaos, the main Lyapunov exponent of the system has been computed as

$$\Lambda = \lim_{t\to+\infty} \frac{1}{t} \ln\left[\frac{|\delta x(t)|}{|\delta x(t_0)|}\right], \tag{22}$$

where $\delta x(t)$ is the linear perturbation obeying

$$\delta\ddot{x} - [\beta \mathrm{D}(x_T - \alpha) - x^2]\delta\dot{x} + (1 + 2x\dot{x})\delta x - \beta\dot{x}\mathrm{H}(x_T - \alpha)\delta x_T = 0 \tag{23}$$

around the solution $x(t)$ from Eq. (11). It is known that a positive Lyapunov exponent is an indication of chaos, and the variations of Λ as a function of the gain β are displayed in Fig 4(b). It can then be noted that in Fig 4, both the bifurcation diagram and the Lyapunov exponent indicate the same window of chaotic behavior for the chosen parameters.

It is interesting to note that in the bifurcation diagram, there is a critical point (at $\beta = 0.405$) where a sudden jump of amplitude occurs. This critical point, which arises from a subcritical bifurcation, depicts a boundary between two regions: for $\beta \leq 0.405$, both variables x and y are quasi-sinusoidal oscillations around the fixed point $(0, 0)$, as confirmed by the limit cycles of Figs 5(a) and (b); and for $\beta > 0.405$, the phase portrait of Fig 5(c) unveils that those variables do not display quasi-sinusoidal oscillations anymore. Other two-dimensional projections of the system attractors for different values of β are presented in Figs. 5(d)-(f). At $\beta = 1.4$, the limit-cycle goes around twice before closing, as a consequence of a first period-doubling bifurcation. Another period-doubling bifurcation creates the four-loop cycle shown for $\beta = 1.55$, and after an infinite cascade of such period-doublings, the system is driven to the strange attractor that is shown for $\beta = 1.7$.

V. Conclusion

In this work, we have investigated an OEO with laser-diode and Van der Pol nonlinearities. We have built the experimental system and established the time-domain equations describing its dynamics. The theoretical study has evidenced the emergence of a Hopf bifurcation as the gain of the system is increased, as well as a time trace asymmetry originating from the laser-diode nonlinearity. The interaction of the time-delay and both nonlinearities leads to some dynamical phenomena that are not encountered in the classical OEO [14], [56], such as sub-critical bifurcations and period-doubling routes to chaos. In future research, we will explore the possibility to use the threshold-like diode nonlinearity for the purpose of pulse generation in OEOs [25], [57]. We will also consider as well other types of complex behaviors that can occur when the dimensionality of the system is expanded [58], along with synchronization phenomena [59]–[61]. We intend to investigate in future works the dynamical properties of this novel type of oscillators that widens the perspective of complexity in photonics [62].

References

[1] A. Neyer and E. Voges, "Dynamics of electrooptic bistable devices with delayed feedback," *IEEE J. Quantum Electron.*, vol. QE-18, no. 12, pp. 2009–2015, Dec. 1982.

[2] A. B. Cohen, B. Ravoori, T. E. Murphy, and R. Roy, "Using synchronization for prediction of high-dimensional chaotic dynamics," *Phys. Rev. Lett.*, vol. 101, p. 154102, Oct. 2008.

[3] K. E. Callan, L. Illing, Z. Gao, D. J. Gauthier, and E. Schöll, "Broadband chaos generated by an optoelectronic oscillator," *Phys. Rev. Lett.*, vol. 104, no. 11, p. 113901, Mar. 2010.

[4] D. P. Rosin, K. E. Callan, D. J. Gauthier, and E. Schöll, "Pulse-train solutions and excitability in an optoelectronic oscillator," *Eur. Phys. Lett.*, vol. 96, no. 3, p. 34001, 2011.

[5] B. Ravoori, A. B. Cohen, J. Sun, A. E. Motter, T. E. Murphy, and R. Roy, "Robustness of optimal synchronization in real networks," *Phys. Rev. Lett.*, vol. 107, p. 034102, Jul. 2011.

[6] L. Weicker, T. Erneux, M. Jacquot, Y. Chembo, and L. Larger, "Crenelated fast oscillatory outputs of a two-delay electro-optic oscillator," *Phys. Rev. E, Stat. Phys. Plasmas Fluids Relat. Interdiscip. Top.*, vol. 85, p. 026206, Feb. 2012.

[7] L. Weicker *et al.*, "Strongly asymmetric square waves in a time-delayed system," *Phys. Rev. E, Stat. Phys. Plasmas Fluids Relat. Interdiscip. Top.*, vol. 86, p. 055201, Nov. 2012.

[8] C. R. S. Williams, T. E. Murphy, R. Roy, F. Sorrentino, T. Dahms, and E. Schöll, "Experimental observations of group synchrony in a system of chaotic optoelectronic oscillators," *Phys. Rev. Lett.*, vol. 110, p. 064104, Feb. 2013.

[9] L. Weicker *et al.*, "Slow—Fast dynamics of a time-delayed electro-optic oscillator," *Philos. Trans. Roy. Soc. A, Math., Phys. Eng. Sci.*, vol. 371, no. 1999, p. 20120459, 2013.

[10] G. R. G. Chengui *et al.*, "Theoretical and experimental study of slow-scale Hopf limit-cycles in laser-based wideband optoelectronic oscillators," *J. Opt. Soc. Amer. B, Opt. Phys.*, vol. 31, no. 10, pp. 2310–2316, 2014.

[11] J. Martínez-Llinàs, P. Colet, and T. Erneux, "Tuning the period of square-wave oscillations for delay-coupled optoelectronic systems," *Phys. Rev. E, Stat. Phys. Plasmas Fluids Relat. Interdiscip. Top.*, vol. 89, p. 042908, Apr. 2014.

[12] L. Weicker, T. Erneux, D. P. Rosin, and D. J. Gauthier, "Multirhythmicity in an optoelectronic oscillator with large delay," *Phys. Rev. E, Stat. Phys. Plasmas Fluids Relat. Interdiscip. Top.*, vol. 91, p. 012910, Jan. 2015.

[13] A. F. Talla *et al.*, "Analysis of phase-locking in narrow-band optoelectronic oscillators with intermediate frequency," *IEEE J. Quantum Electron.*, vol. 51, no. 6, Jun. 2015, Art. no. 5000108.

[14] J. H. T. Mbé *et al.*, "Mixed-mode oscillations in slow-fast delayed optoelectronic systems," *Phys. Rev. E, Stat. Phys. Plasmas Fluids Relat. Interdiscip. Top.*, vol. 91, no. 1, p. 012902, 2015.

[15] A. M. Hagerstrom, T. E. Murphy, and R. Roy, "Harvesting entropy and quantifying the transition from noise to chaos in a photon-counting feedback loop," *Proc. Nat. Acad. Sci. USA*, vol. 112, no. 30, pp. 9258–9263, 2015.

[16] G. R. G. Chengui, P. Woafo, and Y. K. Chembo, "The simplest laser-based optoelectronic oscillator: An experimental and theoretical study," *IEEE J. Lightw. Technol.*, vol. 34, no. 3, pp. 873–878, Feb. 1, 2016.

[17] X. Jiang *et al.*, "Electro-optic chaotic system based on the reverse-time chaos theory and a nonlinear hybrid feedback loop," *Opt. Exp.*, vol. 24, pp. 28804–28814, Dec. 2016.

[18] Y. K. Chembo, M. Jacquot, J. M. Dudley, and L. Larger, "Ikeda-like chaos on a dynamically filtered supercontinuum light source," *Phys. Rev. A, Gen. Phys.*, vol. 94, p. 023847, Aug. 2016.

[19] A. F. Talla, R. Martinenghi, P. Woafo, and Y. K. Chembo, "Breather and pulse-package dynamics in multinonlinear electrooptical systems with delayed feedback," *IEEE Photon. J.*, vol. 8, no. 4, Aug. 2016, Art. no. 7803608.

[20] B. Romeira, F. Kong, W. Li, J. M. L. Figueiredo, J. Javaloyes, and J. Yao, "Broadband chaotic signals and breather oscillations in an optoelectronic oscillator incorporating a microwave photonic filter," *J. Lightw. Technol.*, vol. 32, no. 20, pp. 3933–3942, Oct. 15, 2014.

[21] B. Romeira, J. Javaloyes, J. M. L. Figueiredo, C. N. Ironside, H. I. Cantu, and A. E. Kelly, "Delayed feedback dynamics of Liénard-type resonant tunneling-photo-detector optoelectronic oscillators," *IEEE J. Quantum Electron.*, vol. 49, no. 1, pp. 31–42, Jan. 2013.

[22] X. S. Yao and L. Maleki, "High frequency optical subcarrier generator," *Electron. Lett.*, vol. 30, no. 18, pp. 1525–1526, 1994.

[23] J. Yang, Y. Jin-Long, W. Yao-Tian, Z. Li-Tai, and Y. En-Ze, "An optical domain combined dual-loop optoelectronic oscillator," *IEEE Photon. Technol. Lett.*, vol. 19, no. 11, pp. 807–809, Jun. 1, 2007.

[24] Y. K. Chembo, L. Larger, R. Bendoula, and P. Colet, "Effects of gain and bandwidth on the multimode behavior of optoelectronic microwave oscillators," *Opt. Exp.*, vol. 16, no. 12, pp. 9067–9072, 2008.

[25] Y. K. Chembo, A. Hmima, P.-A. Lacourt, L. Larger, and J. M. Dudley, "Generation of ultralow jitter optical pulses using optoelectronic oscillators with time-lens soliton-assisted compression," *J. Lightw. Technol.*, vol. 27, no. 22, pp. 5160–5167, Nov. 15, 2009.

[26] J. M. Kim and D. Cho, "Optoelectronic oscillator stabilized to an intra-loop Fabry–Perot cavity by a dual servo system," *Opt. Exp.*, vol. 18, no. 14, pp. 14905–14912, 2010.

[27] W. Li and J. Yao, "An optically tunable optoelectronic oscillator," *J. Lightw. Technol.*, vol. 28, no. 18, pp. 2640–2645, Sep. 15, 2010.

[28] I. Ozdur, M. Akbulut, N. Hoghooghi, D. Mandridis, M. U. Piracha, and P. J. Delfyett, "Optoelectronic loop design with 1000 finesse Fabry–Perot etalon," *Opt. Lett.*, vol. 35, no. 6, pp. 799–801, 2010.

[29] O. Okusaga *et al.*, "Spurious mode reduction in dual injection-locked optoelectronic oscillators," *Opt. Exp.*, vol. 19, no. 7, pp. 5839–5854, 2011.

[30] M. Nourine, Y. K. Chembo, and L. Larger, "Wideband chaos generation using a delayed oscillator and a two-dimensional nonlinearity induced by a quadrature phase-shift-keying electro-optic modulator," *Opt. Lett.*, vol. 36, pp. 2833–2835, Aug. 2011.

[31] L. Maleki, "The optoelectronic oscillator," *Nature Photon.*, vol. 5, no. 12, pp. 728–730, 2011.

[32] R. M. Nguimdo, Y. K. Chembo, P. Colet, and L. Larger, "On the phase noise performance of nonlinear double-loop optoelectronic microwave oscillators," *IEEE J. Quantum Electron.*, vol. 48, no. 11, pp. 1415–1423, Nov. 2012.

[33] S. Jia *et al.*, "A novel optoelectronic oscillator based on wavelength multiplexing," *IEEE Photon. Technol. Lett.*, vol. 27, no. 2, pp. 213–216, Jan. 15, 2014.

[34] K. Saleh *et al.*, "Phase noise performance comparison between optoelectronic oscillators based on optical delay lines and whispering gallery mode resonators," *Opt. Exp.*, vol. 22, no. 26, pp. 32158–32173, 2014.

[35] Y. Zhang, D. Hou, and J. Zhao, "Long-term frequency stabilization of an optoelectronic oscillator using phase-locked loop," *J. Lightw. Technol.*, vol. 32, no. 13, pp. 2408–2414, Jul. 1, 2014.

[36] A. Argyris *et al.*, "Chaos-based communications at high bit rates using commercial fibre-optic links," *Nature*, vol. 438, pp. 343–346, Nov. 2005.

[37] R. M. Nguimdo, R. Lavrov, P. Colet, M. Jacquot, Y. K. Chembo, and L. Larger, "Effect of fiber dispersion on broadband chaos communications implemented by electro-optic nonlinear delay phase dynamics," *J. Lightw. Technol.*, vol. 28, no. 8, pp. 2688–2696, Sep. 15, 2010.

[38] A. Uchida, *Optical Communication With Chaotic Lasers: Applications of Nonlinear Dynamics and Synchronization*. New York, NY, USA: Wiley, 2012.

[39] L. Appeltant *et al.*, "Information processing using a single dynamical node as complex system," *Nature Commun.*, vol. 2, no. 13, p. 468, Sep. 2011.

[40] Y. Paquot *et al.*, "Optoelectronic reservoir computing," *Sci. Rep.*, vol. 2, no. 287, Feb. 2012, Art. no. 287.

[41] D. Brunner, M. C. Soriano, C. R. Mirasso, and I. Fischer, "Parallel photonic information processing at gigabyte per second data rates using transient states," *Nature Commun.*, vol. 4, p. 1364, Jan. 2013.

[42] F. Duport, A. Smerieri, A. Akrout, M. Haelterman, and S. Massar, "Fully analogue photonic reservoir computer," *Sci. Rep.*, vol. 6, Mar. 2016, Art. no. 22381.

[43] L. Larger, A. Baylón-Fuentes, R. Martinenghi, V. S. Udaltsov, Y. K. Chembo, and M. Jacquot, "High-speed photonic reservoir computing using a time-delay-based architecture: Million words per second classification," *Phys. Rev. X*, vol. 7, p. 011015, Feb. 2017.

[44] L. Larger, "Complexity in electro-optic delay dynamics: Modelling, design and applications," *Philos. Trans. Roy. Soc. A, Math., Phys. Eng. Sci.*, vol. 371, no. 1999, p. 20120464, 2013.

[45] X. Zou *et al.*, "Optoelectronic oscillators (OEOs) to sensing, measurement, and detection," *IEEE J. Quantum Electron.*, vol. 52, no. 1, Jan. 2016, Art. no. 0601116.

[46] T. Erneux, *Applied Delay Differential Equations*. New York, NY, USA: Springer, 2010.

[47] M. Lakshmanan and D. V. Senthilkumar, *Dynamics of Nonlinear Time-Delay Systems*. New York, NY, USA: Springer, 2011.

[48] P. Zhou, S. Pan, D. Zhu, R. Guo, F. Zhang, and Y. Zhao, "A compact optoelectronic oscillator based on an electroabsorption modulated laser," *IEEE Photon. Technol. Lett.*, vol. 26, no. 1, pp. 86–88, Jan. 1, 2014.

[49] C. Y. Chang *et al.*, "A multi-GHz chaotic optoelectronic oscillator based on laser terminal voltage," *Appl. Phys. Lett.*, vol. 108, no. 19, p. 191109, 2016.

[50] C.-Y. Chang *et al.*, "Tunable X-band optoelectronic oscillators based on external-cavity semiconductor lasers," *IEEE J. Quantum Electron.*, vol. 53, no. 3, Jun. 2017, Art. no. 2000406, doi: 10.1109/JQE.2017.2682702.

[51] J. H. Barron-Zambrano and C. Torres-Huitzil, "FPGA implementation of a configurable neuromorphic CPG-based locomotion controller," *Neural Netw.*, vol. 45, pp. 50–61, Sep. 2013.

[52] M. Ignatov, M. Hansen, M. Ziegler, and H. Kohlstedt, "Synchronization of two memristively coupled van der Pol oscillators," *Appl. Phys. Lett.*, vol. 108, no. 8, p. 084105, 2016.

[53] A. Kumar and P. Mohanty, "Autoassociative memory and pattern recognition in micromechanical oscillator network," *Sci. Rep.*, vol. 7, Mar. 2017, Art. no. 411.

[54] M. Ignatov, M. Ziegler, M. Hansen, and H. Kohlstedt, "Memristive stochastic plasticity enables mimicking of neural synchrony: Memristive circuit emulates an optical illusion," *Sci. Adv.*, vol. 3, p. e1700849, Oct. 2017.

[55] S. Tang, R. Vicente, M. C. Chiang, C. R. Mirasso, and J.-M. Liu, "Nonlinear dynamics of semiconductor lasers with mutual optoelectronic coupling," *IEEE J. Sel. Topics Quantum Electron.*, vol. 10, no. 5, pp. 936–943, Sep. 2004.

[56] M. Peil, M. Jacquot, Y. K. Chembo, L. Larger, and T. Erneux, “Routes to chaos and multiple time scale dynamics in broadband bandpass nonlinear delay electro-optic oscillators,” *Phys. Rev. E, Stat. Phys. Plasmas Fluids Relat. Interdiscip. Top.*, vol. 79, p. 026208, Feb. 2009.

[57] T. Davidson, P. Goldgeier, G. Eisenstein, and M. Orenstein, “High spectral purity CW oscillation and pulse generation in optoelectronic microwave oscillator,” *Electron. Lett.*, vol. 35, no. 15, pp. 1260–1261, Jul. 1999.

[58] L. Keuninckx, G. Van der Sande, and J. Danckaert, “Simple two-transistor single-supply resistor–capacitor chaotic oscillator,” *IEEE Trans. Circuits Syst. II, Exp. Briefs*, vol. 62, no. 9, pp. 891–895, Sep. 2015.

[59] Y. C. Kouomou and P. Woafo, “Stability and optimization of chaos synchronization through feedback coupling with delay,” *Phys. Lett. A*, vol. 298, no. 1, pp. 18–28, 2002.

[60] Y. C. Kouomou and P. Woafo, “Cluster synchronization in coupled chaotic semiconductor lasers and application to switching in chaos-secured communication networks,” *Opt. Commun.*, vol. 223, nos. 4–6, pp. 283–293, Aug. 2003.

[61] Y. C. Kouomou and P. Woafo, “Transitions from spatiotemporal chaos to cluster and complete synchronization states in a shift-invariant set of coupled nonlinear oscillators,” *Phys. Rev. E, Stat. Phys. Plasmas Fluids Relat. Interdiscip. Top.*, vol. 67, p. 046205, Apr. 2003.

[62] M. C. Soriano, J. García-Ojalvo, C. R. Mirasso, and I. Fischer, “Complex photonics: Dynamics and applications of delay-coupled semiconductors lasers,” *Rev. Mod. Phys.*, vol. 85, no. 1, pp. 421–470, 2013.

Géraud R. Goune Chengui received the Ph.D. degree in physics from the University of Yaoundé I, Cameroon, in 2017. His current research is focused on the multi-scale nonlinear dynamics of optoelectronic oscillators.

Jimmi H. Talla Mbé received the Ph.D. degree in physics from the University of Yaoundé I, Cameroon, in 2012. In 2012, he was a Post-Doctoral Fellow with the Franche-Comté Electronique, Mécanique, Thermique et Optique-Sciences et Technologies (FEMTO-ST) Institute, Besançon, France. He is currently an Assistant Professor with the University of Dschang, Cameroon. His research interests include nonlinear dynamics, optoelectronics, photonics, optomechanics, and optical metrology.

Alain Francis Talla received the Ph.D. degree in physics from the University of Yaoundé I, Cameroon, in 2017. His research activities are related to the topic of the nonlinear and stochastic dynamics of optoelectronic oscillators with intermediate frequencies.

Paul Woafo received the Ph.D. degree in physics from the University of Yaoundé I in 1992 and the Ph.D. degree in physics in 1997. He is currently a Full Professor with the University of Yaoundé I, and heads the Laboratory of Modeling and Simulation in Engineering, Biomimetics, and Prototypes. He is a Founding Member and a Former President of the Cameroonian Physical Society, the Vice-President of the African Physical Society, and the Dean of the College of Mathematics and Physical Sciences with the Cameroon Academy of Sciences. He is currently a Senior Associate with the International Center for Theoretical Physics and a Georg Forster Fellow of the Humboldt Foundation, Germany. He is an External Member of the Applied Physics Group, Vrije Universiteit Brussel, Belgium. He has authored or co-authored over 200 refereed articles in international journals. His research interests involve the nonlinear and stochastic dynamics in optoelectronics, electro-mechanics, and biological systems. He was a member of the International Union of Pure and Applied Physics Commission for Statistical Physics. He was a recipient of the TWAS Prize for Young Scientists in 2004.

Yanne K. Chembo (SM’12) received the Ph.D. degree in photonics from the University of the Balearic Islands, Palma, Majorca, Spain, in 2006, and the Ph.D. degree in nonlinear dynamics from the University of Yaoundé I, Cameroon, in 2005. From 2007 to 2008, he was a Post-Doctoral Fellow with the Franche-Comté Electronique, Mécanique, Thermique et Optique-Sciences et Technologies (FEMTO-ST) Institute, Besançon, France. In 2009, he was a NASA Post-Doctoral Program Fellow with the Jet Propulsion Laboratory, Quantum Science and Technology Group, California Institute of Technology, Pasadena, CA, USA. From 2010 to 2016, he was a Senior Research Scientist with the Centre National de la Recherche Scientifique (CNRS), France, with affiliation to the FEMTO-ST Institute, where he founded and led the Microwave Photonics Group for Aerospace and Communication Engineering. In 2017, he joined the International GeorgiaTech-CNRS Research Laboratory, Atlanta, GA, USA. He has co-authored over 80 articles in refereed international journals. His research interests involve microwave photonics, optoelectronics, and the applied nonlinear, stochastic, and quantum dynamics of complex photonic systems. He is a Senior Member of the OSA. He is an Associate Editor of the OSA *journal Optics Express*.